IEEE Access
Multidisciplinary | Rapid Review | Open Access Journal

Received June 29, 2021, accepted July 18, 2021, date of publication July 26, 2021, date of current version August 17, 2021.

Digital Object Identifier 10.1109/ACCESS.2021.3099698

Optimal SWIPT in RIS-Aided MIMO Networks

ZIYI YANG AND YU ZHANG
Department of Information and Electronics, Beijing Institute of Technology, Beijing 100086, China
Corresponding author: Yu Zhang (yuzhang@bit.edu.cn)

This work was supported by the National Natural Science Foundation of China under Grant 61620106001.

ABSTRACT The use of simultaneous wireless information and power transfer (SWIPT) is a key enabler of achieving convenience and prolonging the energy supply lifetime of wireless networks. To address the low efficiencies of far-field power transfer, a reconfigurable intelligent surface (RIS) is adopted to enhance the energy harvesting (EH) performance, which can construct a favorable wireless propagation environment. In this paper, we consider an RIS-assisted SWIPT system with wireless transfer from the access point (AP) to multiple-antenna receivers, which include information receivers (IRs) and energy receivers (ERs). First, we formulate the problem of maximizing the minimum rates of the IRs as a nonconvex constrained optimization problem. For ideal and nonideal channels, we propose two different solutions. Second, we simplify the objective function and decompose the problem into several subproblems by using sorting and iterative optimization algorithms. Moreover, under optimal boundary and Karush-Kuhn-Tucker (KKT) conditions, we successfully solve this problem. The simulation results illustrate a promising approach for wireless communication by comparing ideal RIS and unsatisfactory situations with no RIS cases under various conditions.

INDEX TERMS Reconfigurable intelligent surface (RIS), simultaneous wireless information and power transfer (SWIPT), beamforming, alternating optimization.

I. INTRODUCTION

Simultaneous wireless information and power transfer (SWIPT) is a promising approach for providing convenience and prolonging the energy supply lifetime of wireless networks. SWIPT has a significant advantage, as it effectively utilizes radio frequency (RF) signal information and energy.

SWIPT can be applied to different systems, such as ad hoc networks, where each transmitter (TX) is wirelessly powered by power beacons (PBs) and uses the aggregate power received from PBs to transmit to its desired receiver [1]. SWIPT can also be applied to cooperative clustered wireless sensor networks, where energy-constrained relay nodes harvest the ambient RF signal and use the harvested energy to forward the packets from sources to destinations [2]. In orthogonal frequency division multiplexing (OFDM) systems, a joint subcarrier and power allocation-based SWIPT scheme has been proposed [3]. Moreover, SWIPT is also employed in two-way relay (TWR) channels [4]. An underlying cognitive radio (CR) network can also be considered [5].

In communication networks, the distance from the base station (BS) to a device is critical in terms of both information and power transfer. The prospect of integrating wireless power transfer (WPT) with communication networks creates a need for technology to simultaneously transfer both data and power to end devices. To meet this requirement, the concept of SWIPT was introduced in [6] from a theoretical point of view. A comprehensive summary of SWIPT and related ideas, such as WPT, RF-energy harvesting (EH), and interference exploitation, with comparative tables and illustrative figures has been provided [7]. Interference exploitation is introduced with a fundamental analysis of the interference in two user links to provide foundational knowledge of SWIPT and some suggestions on productive areas for further research related to the SWIPT concept. [8] give a method to achieve robust beamforming design under imperfect channel state information, in which the minimum total transmission power is restricted by the attainable secrecy rate and EH.

A brief survey of state-of-the-art models and several practical transceiver architectures is provided in [9]. Moreover, the most crucial link-level and system-level design aspects are elaborated, with a variety of potential solutions and research ideas. We envision that the dual interpretation of RF signals will create new opportunities and challenges requiring substantial research, innovation, and engineering efforts.

The low efficiency of far-field WPT restricts the fundamental rate-energy (R-E) performance trade-off of the SWIPT system. To address this challenge, reconfigurable

The associate editor coordinating the review of this manuscript and approving it for publication was Wei Feng.

intelligent surface (RIS) technology is adopted to enhance the EH performance of SWIPT-aided systems [10].

An RIS is an appealing green, inexpensive solution for fifth-generation (5G) wireless networks and beyond. An RIS is composed of a significant quantity of low-cost, passive, reflecting elements to provide the desired spectrum and energy efficiency.

Moreover, since an RIS is a complementary device in wireless networks, deploying it in existing wireless systems does not require changing their standardization or hardware; the necessary modification of the communication protocols suffices. As a result, the integration of RISs into wireless networks can be transparent to users, thus providing high flexibility and superior compatibility with existing wireless systems [11]. Reflection beamforming by an RIS helps enhance the signal-to-interference-plus-noise ratio (SINR) of the users near the RIS, which enables a more flexible access point (AP) for transmit beamforming to users outside the RIS coverage. Therefore, the total network performance is improved [12]. Furthermore, the asymptotic squared SNR gain in RIS-aided systems is larger than the linear beamforming gain in both massive multiple-input multiple-output (MIMO) and MIMO relay systems [12], [13].

RISs can be applied in many fields, such as secure communication. Information receivers (IRs) are used to receive best-effort secrecy data, and energy receivers (ERs) harvest energy based on the minimum required harvested power [14]–[16]. Moreover, RISs provide a programmable wireless environment for physical layer security [17]–[21] and multiple cell networks [22], [23]. Integrating an RIS with numerous access networks is a cost-effective solution for boosting the spectrum/energy efficiency and enlarging the network coverage/connections. The method includes capacity and data rate analyses, power and spectral optimization, channel estimation, deep learning-based design, and reliability analysis, making it achievable [24].

An RIS-aided SWIPT system was first studied in [25]. Although there are many works on RIS-aided SWIPT systems, to the best of our knowledge, few studies have focused on beamforming optimization of an RIS-aided cell-free MIMO network with SWIPT. In this paper, we investigate beamforming optimization for RIS-aided cell-free MIMO networks. The aim is to have wireless power APs transmit two types of signals to several RISs and ERs with the reflection of RISs. Unfortunately, directly deriving a globally optimal closed-form solution to the formulated nonconvex max-min problem is impossible because of the intricately coupled optimization variables in the objective function and constraints. An alternating optimization algorithm is proposed in our work to overcome the difficulties of the nonconvex natures of the objective function and constraint functions.

This paper incorporates an RIS into SWIPT in wireless sensor networks as a nonconvex constrained optimization problem. The problem of maximizing the minimum rate of the IRs is exploited in two different environmental conditions: the ideal condition and worst-case condition. We decompose the problem into several subproblems by using sorting and iterative optimization algorithms, transform it into a convex optimization problem using the optimal boundary and S-procedure, and then solve it using the Karush-Kuhn-Tucker (KKT) method. Our simulation results show that the proposed algorithm can converge within a few iterations. The numerical analysis provides practical insights into the effect of various system parameters, such as the ER energy bound, total transmit power, and Frobenius norm-bounded uncertainty region size.

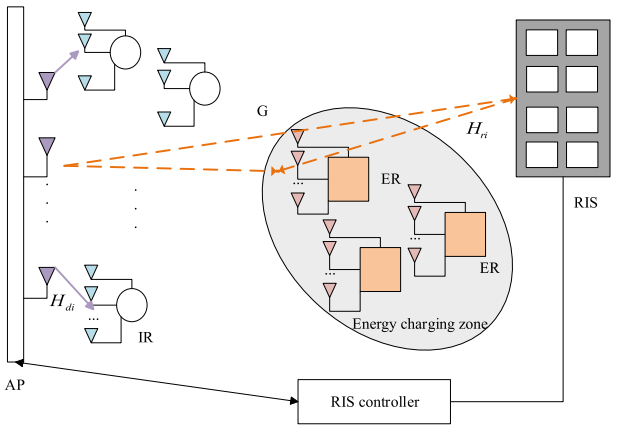

FIGURE 1. RIS-assisted SWIPT system.

II. SYSTEM MODEL

As shown in Figure 1, we consider an RIS-assisted MIMO wireless network, where an RIS with $N_R \in \mathbb{N}^+$ reflecting elements is deployed to assist in SWIPT from an AP with $N_S \in \mathbb{N}^+$ antennas to two sets of multiple-antenna receivers, i.e., $N_I \in \mathbb{N}^+$ antenna IRs and $N_R \in \mathbb{N}^+$ antenna ERs, denoted by the sets $\mathcal{K}_I = \{1, \cdots, K_I\}$, $\mathcal{K}_I \in \mathbb{N}^+$ and $\mathcal{K}_E = \{1, \cdots, K_E\}$, $\mathcal{K}_E \in \mathbb{N}^+$, respectively.

Without loss of generality, we also consider the dedicated information beamforming and energy-carrying signals of each IR and ER. Therefore, the signal transmitted by the BS is defined as

$$\begin{aligned} \boldsymbol{x} &= \sum_{i_I=1}^{K_I} \boldsymbol{v}_{i_I} s_{i_I} + \sum_{i_E=1}^{K_E} \boldsymbol{w}_{i_E} s_{i_E} \\ &= \sum_{i_I=1}^{K_I} \boldsymbol{v}_{i_I} s_{i_I} + \sum_{i_E=1}^{K_E} \boldsymbol{x}_{i_E}, \end{aligned} \tag{1}$$

where s_{i_I} and $s_{i_E} \in \mathbb{C}^{N_S \times 1}$ denote the information symbol for IR i_I and the energy-carrying signal vector for ER i_E, respectively, both of which are assumed to be i.i.d. complex Gaussian distributed, i.e., $s_{i_I} \sim \mathcal{CN}(0, 1)$ and $\boldsymbol{x}_{i_E} \sim \mathcal{CN}(\boldsymbol{0}, \boldsymbol{Q}_{i_E})$, where $\boldsymbol{Q}_{i_E}$ is the energy covariance matrix. The vectors $\boldsymbol{v}_{i_I}$ and $\boldsymbol{w}_{i_E}$ are the corresponding beamforming vectors for s_{i_I} and s_{i_E}.

Furthermore, assume that the AP has a total budget of P_{con}. The transmit power constraint at the BS is expressed as

$$S = E\left(\boldsymbol{x}^{\boldsymbol{H}}\boldsymbol{x}\right) = \sum_{i_I \in \mathcal{K}_I} \|\boldsymbol{v}_{i_I}\|^2 + \sum_{i_E \in \mathcal{K}_E} \mathrm{tr}(\boldsymbol{Q}_{i_E}) \le P_{con},$$

where $\boldsymbol{v}_{i_I} \in \mathbb{C}^{N_S \times 1}$ represents the dedicated beamforming vector for IR i_I. $\boldsymbol{Q}_{i_E} \in \mathbb{C}^{N_R \times 1}$ represents the dedicated beamforming vector for IR i_E.

We assume that the proposed robust transceiver designs in our work are performed at the BS due to its high computational capability. Moreover, the quasistatic flat-fading model is adopted for all channels, with channel reciprocity established for uplink-training-aided downlink channel estimation. In practice, accurate channel state information (CSI) is generally available at the receiver using a high-signal-to-noise-ratio (SNR) training transmission. Simultaneously, the transmitter obtaining perfect CSI is more difficult due to the possible feedback delay and quantization error.

We consider the more realistic case in which the BS has ideal knowledge of the channels from the BS to the RIS and all mobile units (MUs) by utilizing channel reciprocity. In contrast, the channels from the RIS to the MUs are subject to certain errors when feeding back to the BS. Specifically, let us denote the baseband channels from the BS to ER i_E (IR i_R), from the BS to the RIS and from the RIS to ER i_E (IR i_R) by $\boldsymbol{H}_{d,i_E}$ ($\boldsymbol{h}_{d,i_R}^H$), $\boldsymbol{G}$ and $\boldsymbol{H}_{r,i_E}$ ($\boldsymbol{h}_{r,i_I}^H$), respectively. We model imperfect channels $\boldsymbol{H}_{r,i_E}$ and $\boldsymbol{h}_{r,i_I}$ as

$$\begin{aligned} \boldsymbol{H}_{r,i_E} &= \widehat{\boldsymbol{H}}_{r,i_E} + \Delta\boldsymbol{H}_{r,i_E}, \\ \boldsymbol{h}_{r,i_I} &= \widehat{\boldsymbol{h}}_{r,i_I} + \Delta\boldsymbol{h}_{r,i_I}, \\ i_I &\in \mathcal{K}_I, \quad i_E \in \mathcal{K}_E. \end{aligned} \tag{2}$$

According to (2), actual channels $\boldsymbol{H}_{r,i_E}$ and $\boldsymbol{h}_{r,i_I}$ clearly lie in the neighborhoods (also referred to as error regions) of nominal channels $\widehat{\boldsymbol{H}}_{r,i_E}$ and $\widehat{\boldsymbol{h}}_{r,i_I}$, respectively.

In this paper, we mainly consider two different types of CSI errors: $\Delta\boldsymbol{H}_{r,i_E}$ and $\Delta\boldsymbol{h}_{r,i_I}$. Specifically, for deterministically imperfect CSI, Frobenius norm-bounded error regions Ξ_{r,i_E} and Ξ_{r,i_I} are defined as

$$\begin{aligned} \Xi_{r,i_E} &= \{\Delta\boldsymbol{H}_{r,i_E} : \|\Delta\boldsymbol{H}_{r,i_E}\|_F^2 \le \epsilon_{i_E}\}, \\ \Xi_{r,i_I} &= \{\Delta\boldsymbol{h}_{r,i_I} : \|\Delta\boldsymbol{h}_{r,i_I}\|_F^2 \le \epsilon_{i_I}\}, \end{aligned} \tag{3}$$

where ϵ_{i_E} and ϵ_{i_I} denote the radii of error regions $\boldsymbol{\Xi}_{r,i_E}$ and $\boldsymbol{\Xi}_{r,i_E}$, respectively.

For statistically imperfect CSI, we consider

$$\begin{aligned} \mathrm{vec}(\Delta\boldsymbol{H}_{r,i_E}) &\sim \mathcal{CN}(\boldsymbol{0}, \boldsymbol{C}_{r,i_E}), \\ \mathrm{vec}(\Delta\boldsymbol{h}_{r,i_I}) &\sim \mathcal{CN}(\boldsymbol{0}, \boldsymbol{C}_{r,i_I}), \end{aligned} \tag{4}$$

where complex Gaussian distributed errors $\Delta\boldsymbol{H}_{r,i_E}$ and $\Delta\boldsymbol{h}_{r,i_I}$ have covariance matrices $\boldsymbol{C}_{r,i_I}$ and $\boldsymbol{C}_{r,i_E}$, respectively.

Let the diagonal matrix $\boldsymbol{\Phi}_d = \mathrm{diag}[\beta_1 e^{j\theta_1}, \cdots, \beta_{N_R} e^{j\theta_{N_R}}]$ consist of the reflection coefficients of the RIS, where β_n and θ_n, $n = 1, \cdots, N_R$ denote the reflection amplitude and phase shift, respectively, induced by the nth RIS reflecting element. Note that continuous phase shifts induced by the RIS are considered in our work to characterize the performance limit of the RIS. In practice, for ease of circuit implementation, an RIS with discrete phase shifts ranging from 0 to 2π is usually adopted. Since it is costly to simultaneously adjust the reflection amplitude and phase shift of the nth RIS element, we also assume $\beta_n = 1$ to maximize the signal reflection. We set $\gamma_n = 1, n \in N$ to maximize the signal reflection of the RIS. Thus, the signal received at IR $i_I \in \mathcal{K}_I$ is given by

$$\begin{aligned} y_{i_I} &= \boldsymbol{h}_{i_I}^H \boldsymbol{x} + n_{i_I} \\ &= \sum_{j_I \in \mathcal{K}} \boldsymbol{h}_{i_I}^H \boldsymbol{v}_{j_I} s_{j_I} + \sum_{i_E \in \mathcal{K}_E} \boldsymbol{h}_{i_I}^H \boldsymbol{w}_{j_E} s_{i_E} + n_{i_I}, \end{aligned} \tag{5}$$

where $\boldsymbol{H}_{i_E} = \boldsymbol{H}_{d,i_E} + \boldsymbol{H}_{r,i_E}\boldsymbol{\Phi}\boldsymbol{G}$ and $\boldsymbol{h}_{i_I}^H = \boldsymbol{h}_{d,i_I}^H + \boldsymbol{h}_{r,i_I}^H\boldsymbol{\Phi}\boldsymbol{G}$. Moreover, $\boldsymbol{n}_i \sim \mathcal{CN}(\boldsymbol{0}, \boldsymbol{I}_{N_D})$ and $\boldsymbol{n}_i \sim \mathcal{CN}(\boldsymbol{0}, \boldsymbol{I}_{N_D})$ represent the additive white Gaussian noise (AWGN) at ER E_i and IR i_I, respectively.

Under the assumption that IRs are not capable of canceling the interference caused by energy signals, the SINR of IR i_I is given by

$$\mathrm{SINR}_{i_I} = \frac{|\boldsymbol{h}_{i_I}^H \boldsymbol{v}_{i_I}|^2}{\sum\limits_{j_I \ne i_I} |\boldsymbol{h}_{i_I}^H \boldsymbol{v}_{j_I}|^2 + \sum\limits_{i_E \in \mathcal{K}_E} \boldsymbol{h}_{i_I}^H \boldsymbol{Q}_{i_E} \boldsymbol{h}_{i_I} + \sigma_{i_I}^2}. \tag{6}$$

Furthermore, due to the broadcasting nature of wireless channels, ER i_E can harvest energy from all information and energy-carrying signals transmitted by the BS. Hence, the harvested power at ER i_E when neglecting the sufficiently small noise power is presented as

$$E_{i_E} = \eta_{i_E}\Big(\sum_{i_I \in \mathcal{K}_I} \mathrm{tr}(\boldsymbol{H}_{i_E}\boldsymbol{V}_{i_I}\boldsymbol{H}_{i_E}^H) + \sum_{i_E \in \mathcal{K}_E} \mathrm{tr}(\boldsymbol{H}_{i_E}\boldsymbol{Q}_{i_E}\boldsymbol{H}_{i_E}^H)\Big), \tag{7}$$

where $\boldsymbol{V}_{i_I} = \boldsymbol{v}_{i_I}\boldsymbol{v}_{i_I}^H$ and η_{i_E} denotes the EH efficiency at ER i_E.

With both the transmit power constraint and the EH restriction, the beamforming optimization problem is expressed as follows:

$$\begin{aligned} \max_{\boldsymbol{v},\boldsymbol{Q},\boldsymbol{\Phi}} \ & \min_{i_I \in \mathcal{K}_I} \log_2\left(1 + \mathrm{SINR}_{i_I}\right) \\ s.t. \ \ & \mathrm{CR1}: \sum_{i_I \in \mathcal{K}_I} \|\boldsymbol{v}_{i_I}\|^2 + \sum_{i_E \in \mathcal{K}_E} \mathrm{tr}(\boldsymbol{Q}_{i_E}) \le P_\varepsilon \\ & \mathrm{CR2}: E_{i_E} = \eta_{i_E}\Bigg(\sum_{i_I \in \mathcal{K}_I} \mathrm{tr}(\boldsymbol{H}_{i_E}\boldsymbol{V}_{i_I}\boldsymbol{H}_{i_E}^H) \\ & \quad + \sum_{i_E \in \mathcal{K}_E} \mathrm{tr}(\boldsymbol{H}_{i_E}\boldsymbol{Q}_{i_E}\boldsymbol{H}_{i_E}^H)\Bigg) \ge E_{con} \\ & \mathrm{CR3}: |\theta_n| = 1, \quad n \in \{1, 2, \ldots, N_R\}. \end{aligned} \tag{8}$$

which is equivalent to (9), as shown at the bottom of the next page.

III. PROPOSED SOLUTIONS

In this section, we consider ideal and worst-case channel conditions separately solved with an alternating optimization algorithm.

A. EQUIVALENT TRANSFORMATION OF THE PROBLEM

According to the sorting algorithm, we sort the channel gains as $0 < |\bar{\boldsymbol{h}}_1|^2 \leq |\bar{\boldsymbol{h}}_2|^2 \leq \ldots \leq |\bar{\boldsymbol{h}}_{K_I}|^2$. The corresponding serial numbers are $\{\bar{n}_1, \bar{n}_2, \ldots, \bar{n}_{K_I}\}$. To further facilitate addressing problem (9), we propose the following theorem to simplify its objective function.

Theorem 1 is shown at the bottom of the next page.

Proof: According to (9), we define the function

$$f(x) = log_2\left(1 + \frac{Ax}{Bx + \sigma_{i_I}^2}\right), \tag{11}$$

where $A = \boldsymbol{V}_{i_I}$ and $B = \sum_{j_I \in \mathcal{K}_I} \boldsymbol{V}_{j_I} + \sum_{i_E \in \mathcal{K}_E} \boldsymbol{Q}_{i_E} - \boldsymbol{V}_{i_I}$. The first-order derivative of $f(x)$ with respect to x is a monotonically increasing function, and $\frac{df(x)}{dx} > 0$. Therefore, the proof is completed.

Through theorem 1, we can translate (9) into

$$\begin{aligned}
&\max_{\boldsymbol{v},\boldsymbol{Q},\boldsymbol{\Phi}} \frac{\bar{\boldsymbol{h}}_1^H \boldsymbol{V}_{\bar{n}_1} \bar{\boldsymbol{h}}_1}{\sum_{j_I \in \mathcal{K}_I} |\boldsymbol{h}_{i_I}^H \boldsymbol{v}_{j_I}|^2 + \sum_{i_E \in \mathcal{K}_E} \boldsymbol{h}_{i_I}^H \boldsymbol{Q}_{i_E} \boldsymbol{h}_{i_I} - \bar{\boldsymbol{h}}_1^H \boldsymbol{V}_{\bar{n}_1} \bar{\boldsymbol{h}}_1 + \sigma_{i_I}^2} \\
&s.t.\ \ \text{CR1:} \sum_{i_I \in \mathcal{K}_I} \|\boldsymbol{v}_{i_I}\|^2 + \sum_{i_E \in \mathcal{K}_E} \text{tr}(\boldsymbol{Q}_{i_E}) \leq P_\varepsilon \\
&\quad \text{CR2:}\ E_{i_E} = \eta_{i_E}\Big(\sum_{i_I \in \mathcal{K}_I} \text{tr}(\boldsymbol{H}_{i_E} \boldsymbol{V}_{i_I} \boldsymbol{H}_{i_E}^H) \\
&\quad + \sum_{i_E \in \mathcal{K}_E} \text{tr}(\boldsymbol{H}_{i_E} \boldsymbol{Q}_{i_E} \boldsymbol{H}_{i_E}^H)\Big) \geq E_{con} \\
&\quad \text{CR3}: |\theta_n| = 1, \quad n \in \{1, 2, \ldots, N_R\}.
\end{aligned} \tag{12}$$

We use an alternating optimization method in which the AP and RIS independently adjust the transmit beamforming vectors and phase shifts in an alternating manner until convergence is reached. The complexity of this step is $\mathcal{O}(K_I)^2$.

B. OPTIMIZATION OF V AND Q

When we assume that $\boldsymbol{\Phi}$ is perceived, (9) can be translated into

$$\begin{aligned}
&\max_{\boldsymbol{v},\boldsymbol{Q}} \frac{\bar{\boldsymbol{h}}_1^H \boldsymbol{V}_{\bar{n}_1} \bar{\boldsymbol{h}}_1}{\sum_{j_I \in \mathcal{K}_I} |\boldsymbol{h}_{i_I}^H \boldsymbol{v}_{j_I}|^2 + \sum_{i_E \in \mathcal{K}_E} \boldsymbol{h}_{i_I}^H \boldsymbol{Q}_{i_E} \boldsymbol{h}_{i_I} - \bar{\boldsymbol{h}}_1^H \boldsymbol{V}_{\bar{n}_1} \bar{\boldsymbol{h}}_1 + \sigma_{i_I}^2} \\
&s.t.\ \ \text{CR1:} \sum_{i_I \in \mathcal{K}_I} \|\boldsymbol{v}_{i_I}\|^2 + \sum_{i_E \in \mathcal{K}_E} \text{tr}(\boldsymbol{Q}_{i_E}) \leq P_\varepsilon \\
&\quad \text{CR2:}\ E_{i_E} = \eta_{i_E}\Big(\sum_{i_I \in \mathcal{K}_I} \text{tr}(\boldsymbol{H}_{i_E} \boldsymbol{V}_{i_I} \boldsymbol{H}_{i_E}^H) \\
&\quad + \sum_{i_E \in \mathcal{K}_E} \text{tr}(\boldsymbol{H}_{i_E} \boldsymbol{Q}_{i_E} \boldsymbol{H}_{i_E}^H)\Big) \geq E_{con}.
\end{aligned} \tag{13}$$

By introducing the auxiliary variable μ, equation (13) can be written as

$$\begin{aligned}
&\max_{\boldsymbol{v},\boldsymbol{Q}} \frac{\mu}{\sum_{j_I \in \mathcal{K}_I} |\boldsymbol{h}_{i_I}^H \boldsymbol{v}_{j_I}|^2 + \sum_{i_E \in \mathcal{K}_E} \boldsymbol{h}_{i_I}^H \boldsymbol{Q}_{i_E} \boldsymbol{h}_{i_I} - \mu + \sigma_{i_I}^2} \\
&s.t.\ \ \text{CR1:} \sum_{i_I \in \mathcal{K}_I} \|\boldsymbol{v}_{i_I}\|^2 + \sum_{i_E \in \mathcal{K}_E} \text{tr}(\boldsymbol{Q}_{i_E}) \leq P_\varepsilon \\
&\quad \text{CR2:}\ E_{i_E} = \mu_{i_E}\Big(\sum_{i_I \in \mathcal{K}_I} \text{tr}(\boldsymbol{H}_{i_E} \boldsymbol{V}_{i_I} \boldsymbol{H}_{i_E}^H) \\
&\quad + \sum_{i_E \in \mathcal{K}_E} \text{tr}(\boldsymbol{H}_{i_E} \boldsymbol{Q}_{i_E} \boldsymbol{H}_{i_E}^H)\Big) \geq E_{con} \\
&\quad \text{CR3:}\ \mu \leq \bar{\boldsymbol{h}}_1^H \boldsymbol{V}_{\bar{n}_1} \bar{\boldsymbol{h}}_1.
\end{aligned} \tag{14}$$

1) PERFECT CONDITION

When the channel of IRs and ERs is ideal, we can readily achieve $\boldsymbol{\sigma}^2 = 0, \boldsymbol{V}(i,j) = 0, \boldsymbol{Q}(i,j) = 0$ while $i \neq j$. (14) is transformed into

$$\min_{\boldsymbol{V},\boldsymbol{Q}} \Big(\sum_{j_I \in \mathcal{K}_I} \boldsymbol{h}_{i_I}^H \boldsymbol{V}_{j_I} \boldsymbol{h}_{i_I} + \sum_{i_E \in \mathcal{K}_E} \boldsymbol{h}_{i_I}^H \boldsymbol{Q}_{i_E} \boldsymbol{h}_{i_I}\Big)/\mu \tag{15a}$$

$$s.t.\ \ \text{CR1:} \sum_{i_I \in \mathcal{K}_I} \text{tr}(\boldsymbol{V}_{i_I}) + \sum_{i_E \in \mathcal{K}_E} \text{tr}(\boldsymbol{Q}_{i_E}) \leq P_\varepsilon \tag{15b}$$

$$\text{CR2:}\ E_{i_E} = \eta_{i_E}\Big(\sum_{i_I \in \mathcal{K}_I} \text{tr}(\boldsymbol{H}_{i_E} \boldsymbol{V}_{i_I} \boldsymbol{H}_{i_E}^H) + \sum_{i_E \in \mathcal{K}_E} \text{tr}(\boldsymbol{H}_{i_E} \boldsymbol{Q}_{i_E} \boldsymbol{H}_{i_E}^H)\Big) \geq E_{con} \tag{15c}$$

$$\text{CR3:}\ \mu \leq \bar{\boldsymbol{h}}_1^H \boldsymbol{V}_{\bar{n}_1} \bar{\boldsymbol{h}}_1. \tag{15d}$$

When we consider the functions of $\boldsymbol{V}$ and $\boldsymbol{Q}$, they can be interpreted as convex functions that can be resolved by the CVX or KKT condition method. Through the KKT conditions, we obtain the closed-form solution of (15a).

Next, we focus our attention on optimization of (15d) and use the water injection theorem. When every $\boldsymbol{h}_{i_I}^H \boldsymbol{V}_{i_I} \boldsymbol{h}_{i_I}$ and $\boldsymbol{h}_{i_I}^H \boldsymbol{Q}_{i_I} \boldsymbol{h}_{i_I}$ is equal, we achieve the maximum of (8).

Proof 1: Please refer to Appendix A.

$$\begin{aligned}
&\max_{\boldsymbol{v},\boldsymbol{Q}} \min_{i_I \in \mathcal{K}_I} \log_2\left(1 + \frac{\boldsymbol{h}_{i_I}^H \boldsymbol{V}_{i_I} \boldsymbol{h}_{i_I}}{\sum_{j_I \in \mathcal{K}_I} |\boldsymbol{h}_{i_I}^H \boldsymbol{v}_{j_I}|^2 + \sum_{i_E \in \mathcal{K}_E} \boldsymbol{h}_{i_I}^H \boldsymbol{Q}_{i_E} \boldsymbol{h}_{i_I} - \boldsymbol{h}_{i_I}^H \boldsymbol{V}_{i_I} \boldsymbol{h}_{i_I} + \sigma_{i_I}^2}\right) \\
&s.t.\ \ \text{CR1:} \sum_{i_I \in \mathcal{K}_I} \|\boldsymbol{v}_{i_I}\|^2 + \sum_{i_E \in \mathcal{K}_E} \text{tr}(\boldsymbol{Q}_{i_E}) \leq P_\varepsilon \\
&\quad \text{CR2:}\ E_{i_E} = \eta_{i_E}\Big(\sum_{i_I \in \mathcal{K}_I} \text{tr}(\boldsymbol{H}_{i_E} \boldsymbol{V}_{i_I} \boldsymbol{H}_{i_E}^H) + \sum_{i_E \in \mathcal{K}_E} \text{tr}(\boldsymbol{H}_{i_E} \boldsymbol{Q}_{i_E} \boldsymbol{H}_{i_E}^H)\Big) \geq E_{con}
\end{aligned} \tag{9}$$

We conclude that this alternating optimization algorithm converges with complexity $N_S\mathcal{K}_I$.

2) IMPERFECT SITUATION

When considering an unsatisfactory situation, we utilize the same system setup as that in the perfect case. We additionally define the imperfect IR and ER channels as

$$\begin{aligned}\mathbf{h} &= \widehat{\mathbf{h}} + \Delta\mathbf{h},\\ \bar{\boldsymbol{h}}_1 &= \hat{\mathbf{h}}_1 + \Delta\bar{\mathbf{h}}_1,\end{aligned} \tag{16}$$

where $\widehat{\mathbf{h}}_k$ is the nominal channel, and $\Delta\mathbf{h}$ is the deterministically bounded CSI error, i.e., $\|\Delta\boldsymbol{H}_{i_E}\|_F^2 \le \epsilon_{i_E}$, $\|\Delta\boldsymbol{h}_{i_I}\|_F^2 \le \epsilon_{i_I}$, where ϵ denotes the Frobenius norm-bounded uncertainty region size.

The corresponding problem is then formulated as

$$\begin{aligned}\max_{\boldsymbol{V},\boldsymbol{Q}}\ & \log_2\left(1+\frac{|\bar{\boldsymbol{h}}_1^H\boldsymbol{v}_{\bar{n}_1}|^2}{\sum\limits_{j_I\neq\bar{n}_1}|\boldsymbol{h}_{i_I}^H\boldsymbol{v}_{j_I}|^2+\sum\limits_{i_E\in\mathcal{K}_E}\boldsymbol{h}_{i_I}^H\boldsymbol{Q}_{i_E}\boldsymbol{h}_{i_I}+\sigma_{i_I}^2}\right)\\ s.t.\ \ &\text{CR1: } \boldsymbol{H}_{i_E}=\widehat{\boldsymbol{H}}_{i_E}+\Delta\boldsymbol{H}_{i_E},\quad \boldsymbol{h}_{i_I}=\widehat{\boldsymbol{h}}_{i_I}+\Delta\boldsymbol{h}_{i_I}\\ &\text{CR2: } \sum_{i_I\in\mathcal{K}_I}\|\boldsymbol{v}_{i_I}\|^2+\sum_{i_E\in\mathcal{K}_E}\mathrm{tr}(\boldsymbol{Q}_{i_E})\le P_\varepsilon\\ &\text{CR3: } E_{i_E}=\eta_{i_E}\Big(\sum_{i_I\in\mathcal{K}_I}\mathrm{tr}(\boldsymbol{H}_{i_E}\boldsymbol{V}_{i_I}\boldsymbol{H}_{i_E}^H)\\ &+\sum_{i_E\in\mathcal{K}_E}\mathrm{tr}(\boldsymbol{H}_{i_E}\boldsymbol{Q}_{i_E}\boldsymbol{H}_{i_E}^H)\Big)\ge E_{con}\\ &\text{CR4: } \|\Delta\boldsymbol{H}_{i_E}\|_F^2\le\epsilon_{i_E},\quad \|\Delta\boldsymbol{h}_{i_I}\|_F^2\le\epsilon_{i_I}.\end{aligned} \tag{17}$$

We substitute CR1 into the objective function and CR2 to obtain formula (18), as shown at the bottom of the next page.

Similar to the perfect case, by inputting the auxiliary variable μ, we convert problem (13) into (19), as shown at the bottom of the next page, on the following page.

To solve problem (19), we introduce the following lemma.

Lemma 1 (S-Procedure): Assume $f(\mathbf{x}) = \mathbf{x}^H\mathbf{A}\mathbf{x}+\mathbf{x}^H\mathbf{b}+\mathbf{b}^H\mathbf{x}+c$, *where* $\mathbf{x}\in\mathbb{C}^N$, $\mathbf{A}\in\mathbb{H}^{N\times N}$, $\mathbf{b}\in\mathbb{C}^N$, *and* c *is a constant. Subsequently, the following equivalence holds*:

$$\begin{aligned}&f(\mathbf{x})\le 0,\quad \forall\mathbf{x}\in\{\mathbf{x}\mid tr(\mathbf{x}\mathbf{x}^H)\le\epsilon_e\}\\ &\Leftrightarrow u\begin{bmatrix}\mathbf{I}_N & \mathbf{0}_{N\times1}\\ \mathbf{0}_{N\times1}^T & -\epsilon_e\end{bmatrix}-\begin{bmatrix}\mathbf{A} & \mathbf{b}\\ \mathbf{b}^H & c\end{bmatrix}\succeq\mathbf{0},\\ &\quad \textit{with some}\ \ u\ge 0.\end{aligned} \tag{20}$$

Applying Lemma 1, we can reformulate (19d) as

$$\begin{aligned}&\begin{bmatrix}u_1\mathbf{I}_N+\boldsymbol{V}_{\bar{n}_1} & \boldsymbol{V}_{\bar{n}_1}\hat{\mathbf{h}}_1\\ \hat{\mathbf{h}}_1^H\boldsymbol{V}_{\bar{n}_1} & -\mu-\epsilon_{i_I}-\hat{\mathbf{h}}_1^H\boldsymbol{V}_{\bar{n}_1}\hat{\mathbf{h}}_1\end{bmatrix}\succeq\mathbf{0},\\ &u_1\ge 0.\end{aligned} \tag{21}$$

(21) can be regarded as a convex linear matrix inequality (LMI).

$$\begin{aligned}\min_{\boldsymbol{V},\boldsymbol{Q}}\ &\Big(\sum_{j_I\in\mathcal{K}_I}(\widehat{\boldsymbol{h}}_{i_E}+\Delta\boldsymbol{h}_{i_E})^H\boldsymbol{V}_{j_I}(\widehat{\boldsymbol{h}}_{i_E}+\Delta\boldsymbol{h}_{i_E})\\ &+\sum_{i_E\in\mathcal{K}_E}(\widehat{\boldsymbol{h}}_{i_E}+\Delta\boldsymbol{h}_{i_E})^H\boldsymbol{Q}_{i_E}(\widehat{\boldsymbol{h}}_{i_E}+\Delta\boldsymbol{h}_{i_E})+\sigma_{i_I}^2\Big)/\mu\end{aligned} \tag{22a}$$

$$s.t.\ \ \text{CR1: } \sum_{i_I\in\mathcal{K}_I}\|\boldsymbol{v}_{i_I}\|^2+\sum_{i_E\in\mathcal{K}_E}\mathrm{tr}(\boldsymbol{Q}_{i_E})\le P_\varepsilon \tag{22b}$$

$$\begin{aligned}&\text{CR2: } \eta_{i_E}\Big(\sum_{i_I\in\mathcal{K}_I}\mathrm{tr}((\widehat{\boldsymbol{H}}_{i_E}+\Delta\boldsymbol{H}_{i_E})\boldsymbol{V}_{i_I}(\widehat{\boldsymbol{H}}_{i_E}+\Delta\boldsymbol{H}_{i_E})^H)\\ &+\sum_{i_E\in\mathcal{K}_E}\mathrm{tr}((\widehat{\boldsymbol{H}}_{i_E}+\Delta\boldsymbol{H}_{i_E})\boldsymbol{Q}_{i_E}(\widehat{\boldsymbol{H}}_{i_E}+\Delta\boldsymbol{H}_{i_E})^H)\Big)\ge E_{con}\end{aligned} \tag{22c}$$

$$\begin{aligned}&\text{CR3: } \begin{bmatrix}u_1\mathbf{I}_N+\boldsymbol{V}_{\bar{n}_1} & \boldsymbol{V}_{\bar{n}_1}\hat{\mathbf{h}}_1\\ \hat{\mathbf{h}}_1^H\boldsymbol{V}_{\bar{n}_1} & -\mu-\epsilon_{i_I}-\hat{\mathbf{h}}_1^H\boldsymbol{V}_{\bar{n}_1}\hat{\mathbf{h}}_1\end{bmatrix}\succeq\mathbf{0},\\ &u_1\ge 0.\end{aligned} \tag{22d}$$

Given any feasible μ, problem (22) is jointly concave and can thus be globally solved by golden section search (GSS). Additionally, we prove that problem (22) is quasiconcave. The error $\boldsymbol{H}_E, \boldsymbol{h}_I$ in the equivalent problem (22) is actually independent of η. Based on the above discussion, the proposed semidefinite programming (SDP)-based linear search for solving problem (15) can obviously be directly extended to problem (22).

As a result, we can reformulate (22) as

$$\begin{aligned}\min_{\boldsymbol{V},\boldsymbol{Q}}\ &\Big(\sum_{j_I\in\mathcal{K}_I}(\widehat{\boldsymbol{h}}_{i_E}+\Delta\boldsymbol{h}_{i_E})^H\boldsymbol{V}_{j_I}(\widehat{\boldsymbol{h}}_{i_E}+\Delta\boldsymbol{h}_{i_E})\\ &+\sum_{i_E\in\mathcal{K}_E}(\widehat{\boldsymbol{h}}_{i_E}+\Delta\boldsymbol{h}_{i_E})^H\boldsymbol{Q}_{i_E}(\widehat{\boldsymbol{h}}_{i_E}+\Delta\boldsymbol{h}_{i_E})+\sigma_{i_I}^2\Big)/\mu\end{aligned} \tag{23a}$$

Theorem 1: For all IRs,

$$\begin{aligned}&\min_{i_I\in\mathcal{K}_I}\log_2\left(1+\frac{\boldsymbol{h}_{i_I}^H\boldsymbol{V}_{i_I}\boldsymbol{h}_{i_I}}{\sum\limits_{j_I\in\mathcal{K}_I}|\boldsymbol{h}_{i_I}^H\boldsymbol{v}_{j_I}|^2+\sum\limits_{i_E\in\mathcal{K}_E}\boldsymbol{h}_{i_I}^H\boldsymbol{Q}_{i_E}\boldsymbol{h}_{i_I}-\boldsymbol{h}_{i_I}^H\boldsymbol{V}_{i_I}\boldsymbol{h}_{i_I}+\sigma_{i_I}^2}\right)\\ &=\log_2\left(1+\frac{\bar{\boldsymbol{h}}_1^H\boldsymbol{V}_{\bar{n}_1}\bar{\boldsymbol{h}}_1}{\sum\limits_{j_I\in\mathcal{K}_I}|\boldsymbol{h}_{i_I}^H\boldsymbol{v}_{j_I}|^2+\sum\limits_{i_E\in\mathcal{K}_E}\boldsymbol{h}_{i_I}^H\boldsymbol{Q}_{i_E}\boldsymbol{h}_{i_I}-\bar{\boldsymbol{h}}_1^H\boldsymbol{V}_{\bar{n}_1}\bar{\boldsymbol{h}}_1+\sigma_{i_I}^2}\right)\end{aligned} \tag{10}$$

$$s.t.\ \text{CR1:}\ \sum_{i_I\in\mathcal{K}_I}\|\boldsymbol{v}_{i_I}\|^2+\sum_{i_E\in\mathcal{K}_E}\text{tr}(\boldsymbol{Q}_{i_E})\le P_\varepsilon \tag{23b}$$

$$\text{CR2:}\ \eta_{i_E}\Bigg(\sum_{i_I\in\mathcal{K}_I}\text{tr}((\widehat{\boldsymbol{H}}_{i_E}+\Delta\boldsymbol{H}_{i_E})\boldsymbol{V}_{i_I}(\widehat{\boldsymbol{H}}_{i_E}+\Delta\boldsymbol{H}_{i_E})^H)+\sum_{i_E\in\mathcal{K}_E}\text{tr}((\widehat{\boldsymbol{H}}_{i_E}+\Delta\boldsymbol{H}_{i_E})\boldsymbol{Q}_{i_E}(\widehat{\boldsymbol{H}}_{i_E}+\Delta\boldsymbol{H}_{i_E})^H)\Bigg)\ge E_{con} \tag{23c}$$

$$\text{CR3:}\ \mathbf{I}_{E_1}+\mathbf{R}_E^H\boldsymbol{V}_{\bar{n}_1}\mathbf{R}_E\succeq\mathbf{0}, \tag{23d}$$

where $\mathbf{I}_{E_1}=\begin{bmatrix}u_1\mathbf{I}_N & 0\\ 0 & -\mu-\epsilon_{i_I}\end{bmatrix}$, $\mathbf{R}_E=\begin{bmatrix}\mathbf{I}\\ \hat{\mathbf{h}}_1\end{bmatrix}$, $u_1\ge 0$.

With the use of KKT conditions, we obtain the closed-form solution of (23a).

When every $(\widehat{\boldsymbol{h}}_{i_E}+\Delta\boldsymbol{h}_{i_E})^H(\boldsymbol{V}+\boldsymbol{Q})(\widehat{\boldsymbol{h}}_{i_E}+\Delta\boldsymbol{h}_{i_E})$ and every $\mathbf{R}_E^H\boldsymbol{V}_{\bar{n}_1}\mathbf{R}_E$ are equal, we achieve the maximum of (17).

Proof 2: Please refer to Appendix B.

$N_S\mathcal{K}_I$ illustrates the complexity of this step.

C. PHASE SHIFT OPTIMIZATION

When we assume that $\boldsymbol{V}$ and $\boldsymbol{Q}$ are known, we express $\tilde{\boldsymbol{h}}=[\boldsymbol{h}_1,\boldsymbol{h}_2,\ldots,\boldsymbol{h}_{K_I}]$, $\boldsymbol{V}_c=\begin{bmatrix}\boldsymbol{V}_1 & 0 & \ldots & 0\\ 0 & \boldsymbol{V}_2 & \ldots & 0\\ & & \cdots & \\ 0 & 0 & \ldots & \boldsymbol{V}_{j_I}\end{bmatrix}$, $\boldsymbol{Q}_c=\begin{bmatrix}\boldsymbol{Q}_1 & 0 & \ldots & 0\\ 0 & \boldsymbol{Q}_2 & \ldots & 0\\ & & \cdots & \\ 0 & 0 & \ldots & \boldsymbol{Q}_{i_E}\end{bmatrix}$, and $\tilde{\boldsymbol{V}}_{\bar{n}_1}=\begin{bmatrix}0 & 0 & \ldots & 0\\ 0 & \ldots & \ldots & 0\\ & \ldots & \boldsymbol{V}_{\bar{n}_1} & \\ 0 & 0 & \ldots & 0\end{bmatrix}$ as partitioned matrices.

We can reformulate (23) as

$$\min_{\boldsymbol{\Phi}}\ \tilde{\boldsymbol{h}}^H\big((\boldsymbol{V}_c+\boldsymbol{Q}_c)/\tilde{\boldsymbol{V}}_{\bar{n}_1}\big)\tilde{\boldsymbol{h}} \tag{24a}$$

$$\text{CR1:}\ 0\le\theta_n\le 2\pi,\quad \forall n=1,\ldots,N. \tag{24b}$$

$$\text{CR2:}\ \mathbf{I}_{E_1}+\mathbf{R}_E^H\tilde{\boldsymbol{V}}_{\bar{n}_1}\mathbf{R}_E\succeq\mathbf{0}. \tag{24c}$$

To maximize (24a), let

$$arg(\boldsymbol{h}_{r,i_I}^H\boldsymbol{\Phi}\boldsymbol{G}\big((\boldsymbol{V}_c+\boldsymbol{Q}_c)/\tilde{\boldsymbol{V}}_{\bar{n}_1}\big)\boldsymbol{h}_{r,i_I}\boldsymbol{\Phi}\boldsymbol{G}) = -arg(\boldsymbol{h}_{d,i_I}^H\big((\boldsymbol{V}_c+\boldsymbol{Q}_c)/\tilde{\boldsymbol{V}}_{\bar{n}_1}\big)\boldsymbol{h}_{d,i_I})=\varphi_0, \tag{25}$$

with $arg(\cdot)$ denoting the component-wise phase of a complex vector. Subsequently, (24a) equals

$$\boldsymbol{h}_{r,i_I}^H\boldsymbol{\Phi}\boldsymbol{G}\big((\boldsymbol{V}_c+\boldsymbol{Q}_c)/\tilde{\boldsymbol{V}}_{\bar{n}_1}\big)\boldsymbol{h}_{r,i_I}\boldsymbol{\Phi}\boldsymbol{G}. \tag{26}$$

We assume

$$\boldsymbol{h}_{r,i_I}^H\boldsymbol{\Phi}\boldsymbol{G}\big((\boldsymbol{V}_c+\boldsymbol{Q}_c)/\tilde{\boldsymbol{V}}_{\bar{n}_1}\big)\boldsymbol{h}_{r,i_I}\boldsymbol{\Phi}\boldsymbol{G}=\boldsymbol{a}^H\boldsymbol{d}, \tag{27}$$

where

$\boldsymbol{a}=[1e^{j\theta_1},\cdots,e^{j\theta_{N_R}}]^H$ and

$\boldsymbol{d}=\text{diag}(\boldsymbol{h}_{r,i_I}^H\boldsymbol{h}_{r,i_I})\boldsymbol{G}\big((\boldsymbol{V}_c+\boldsymbol{Q}_c)/\tilde{\boldsymbol{V}}_{\bar{n}_1}\big)\boldsymbol{G}$.

Problem (24) is reduced to

$$\min_{\boldsymbol{a}}\ \boldsymbol{a}^H\boldsymbol{d} \tag{28a}$$

$$\max_{\boldsymbol{v},\boldsymbol{Q}}\ \log_2\Big(1+\frac{|(\hat{\mathbf{h}}_1+\Delta\bar{\mathbf{h}}_1)^H\boldsymbol{v}_{\bar{n}_1}|^2}{\sum_{j_I\neq\bar{n}_1}|(\widehat{\boldsymbol{h}}_{i_I}+\Delta\boldsymbol{h}_{i_I})^H\boldsymbol{v}_{j_I}|^2+\sum_{i_E\in\mathcal{K}_E}(\widehat{\boldsymbol{h}}_{i_I}+\Delta\boldsymbol{h}_{i_I})^H\boldsymbol{Q}_{i_E}(\widehat{\boldsymbol{h}}_{i_I}+\Delta\boldsymbol{h}_{i_I})+\sigma_{i_I}^2}\Big)$$

$$s.t.\ \text{CR1:}\ \sum_{i_I\in\mathcal{K}_I}\|\boldsymbol{v}_{i_I}\|^2+\sum_{i_E\in\mathcal{K}_E}\text{tr}(\boldsymbol{Q}_{i_E})\le P_\varepsilon$$

$$\text{CR2:}\ E_{i_E}=\eta_{i_E}\Bigg(\sum_{i_I\in\mathcal{K}_I}\text{tr}((\widehat{\boldsymbol{H}}_{i_E}+\Delta\boldsymbol{H}_{i_E})\boldsymbol{V}_{i_I}(\widehat{\boldsymbol{H}}_{i_E}+\Delta\boldsymbol{H}_{i_E})^H)+\sum_{i_E\in\mathcal{K}_E}\text{tr}((\widehat{\boldsymbol{H}}_{i_E}+\Delta\boldsymbol{H}_{i_E})\boldsymbol{Q}_{i_E}(\widehat{\boldsymbol{H}}_{i_E}+\Delta\boldsymbol{H}_{i_E})^H)\Bigg)\ge E_{con}$$

$$\text{CR3:}\ \|\Delta\boldsymbol{H}_{i_E}\|_F^2\le\epsilon_{i_E},\quad \|\Delta\boldsymbol{h}_{i_I}\|_F^2\le\epsilon_{i_I}. \tag{18}$$

$$\max_{\boldsymbol{V},\boldsymbol{Q}}\ \frac{\mu}{\sum_{j_I\in\mathcal{K}_I}(\widehat{\boldsymbol{h}}_{i_E}+\Delta\boldsymbol{h}_{i_E})^H\boldsymbol{V}_{j_I}(\widehat{\boldsymbol{h}}_{i_E}+\Delta\boldsymbol{h}_{i_E})+\sum_{i_E\in\mathcal{K}_E}(\widehat{\boldsymbol{h}}_{i_E}+\Delta\boldsymbol{h}_{i_E})^H\boldsymbol{Q}_{i_E}(\widehat{\boldsymbol{h}}_{i_E}+\Delta\boldsymbol{h}_{i_E})-\mu+\sigma_{i_I}^2} \tag{19a}$$

$$s.t.\ \text{CR1:}\ \sum_{i_I\in\mathcal{K}_I}\|\boldsymbol{v}_{i_I}\|^2+\sum_{i_E\in\mathcal{K}_E}\text{tr}(\boldsymbol{Q}_{i_E})\le P_\varepsilon \tag{19b}$$

$$\text{CR2:}\ \eta_{i_E}\Bigg(\sum_{i_I\in\mathcal{K}_I}\text{tr}((\widehat{\boldsymbol{H}}_{i_E}+\Delta\boldsymbol{H}_{i_E})\boldsymbol{V}_{i_I}(\widehat{\boldsymbol{H}}_{i_E}+\Delta\boldsymbol{H}_{i_E})^H)+\sum_{i_E\in\mathcal{K}_E}\text{tr}((\widehat{\boldsymbol{H}}_{i_E}+\Delta\boldsymbol{H}_{i_E})\boldsymbol{Q}_{i_E}(\widehat{\boldsymbol{H}}_{i_E}+\Delta\boldsymbol{H}_{i_E})^H)\Bigg)\ge E_{con} \tag{19c}$$

$$\text{CR3:}\ \mu\le\min\ (\hat{\mathbf{h}}_1+\Delta\bar{\mathbf{h}}_1)^H\boldsymbol{V}_{\bar{n}_1}(\hat{\mathbf{h}}_1+\Delta\bar{\mathbf{h}}_1) \tag{19d}$$

$$\text{CR4:}\ \|\Delta\boldsymbol{H}_{i_E}\|_F^2\le\epsilon_{i_E},\quad \|\Delta\boldsymbol{h}_{i_I}\|_F^2\le\epsilon_{i_I}. \tag{19e}$$

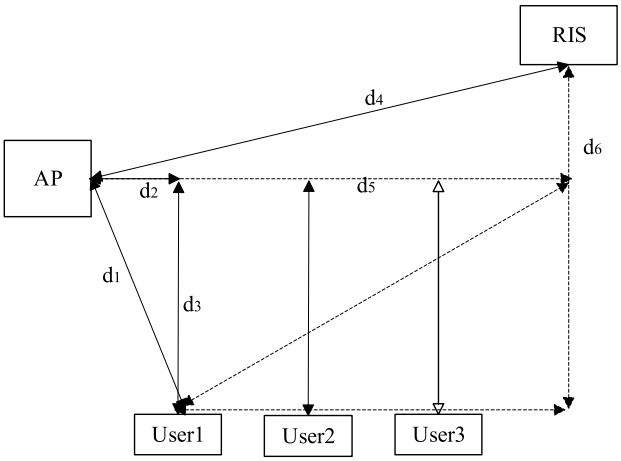

FIGURE 2. Simulation setup.

$$\text{CR1: } |a_n| = 1, \quad \forall n = 1, \ldots, N. \tag{28b}$$
$$\text{CR2: } arg(\boldsymbol{a}^H \boldsymbol{d}) = \varphi_0. \tag{28c}$$

It can be verified that the optimal solution is given by

$$\begin{aligned} \boldsymbol{a}^* &= e^{j(\varphi_0 - arg(\boldsymbol{d}))} \\ &= e^{j(\varphi_0 - arg(\text{diag}(\boldsymbol{h}_{r,i_I}^H \boldsymbol{h}_{r,i_I}) \boldsymbol{G}\left((\boldsymbol{V_c} + \boldsymbol{Q_c})/\tilde{\boldsymbol{V}}_{\tilde{n}_1}\right) \boldsymbol{G})}. \end{aligned} \tag{29}$$

Thus, the corresponding nth phase shift at the RIS is given by

$$\begin{aligned} \theta_n^* &= \varphi_0 - arg(\boldsymbol{h}_{r,i_I}^H \boldsymbol{h}_{r,i_I} \boldsymbol{g}_n^H \left((\boldsymbol{V_c} + \boldsymbol{Q_c})/\tilde{\boldsymbol{V}}_{\tilde{n}_1}\right) \boldsymbol{g}_n) \\ &= \varphi_0 - arg((\boldsymbol{h}_{r,i_I}^H \boldsymbol{h}_{r,i_I}) - arg(\boldsymbol{g}_n^H \left((\boldsymbol{V_c} + \boldsymbol{Q_c})/\tilde{\boldsymbol{V}}_{\tilde{n}_1}\right) \boldsymbol{g}_n), \end{aligned} \tag{30}$$

where $\boldsymbol{g}_n^H$ is the nth row vector of $\boldsymbol{G}$.

IV. SIMULATION RESULTS AND DISCUSSION

In this section, we consider a uniform linear array (ULA) at the AP and a uniform rectangular array (URA) at the RIS with $N = N_x * N_y$, where N_x and N_y denote the number of reflecting elements in the horizontal direction and vertical direction, respectively. The ULA is positioned in parallel to the URA at the same altitude. The location of the AP and the location of the RIS are (0, 20) m and (40, 30) m, respectively. In addition, the users are assumed to be located at (10, 0) m, (20, 0) m and (30, 0) m. This situation is shown in Fig. 2. The AP-user1 distance and RIS-user1 link distance are given by $d_1 = \sqrt{d_2^2 + d_3^2}$ and $d_4 = \sqrt{d_5^2 + d_6^2}$, respectively. The distances between the AP and the RIS and between User 2 and User 3 can be easily obtained.

We can quickly obtain the distances between the APs and RISs and between users. In the considered large-scale fading model, the BS-RIS-user link suffers the double-fading effect, which gives us access to an ideal system model. According to these settings, we assume that the CSI is available. The signal attenuation at a reference distance of 1 m is set to 30 dB for all channels. The antenna gain of both the AP and users is assumed to be 40 dBi [26]. According to these settings, we assume that all wireless channel coefficients follow the

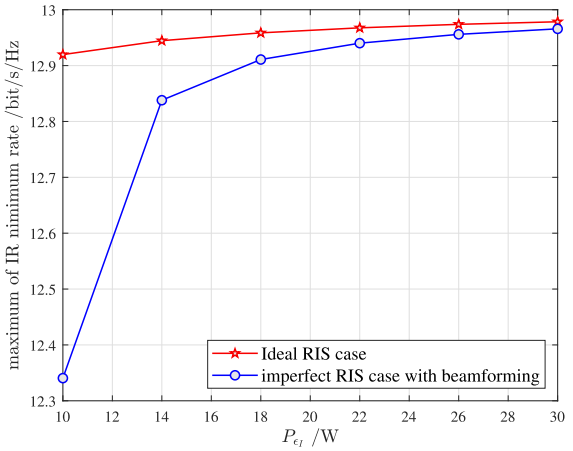

FIGURE 3. Maximum IR minimum rate over P_{ε_I} when $\sigma_n^2 = -140$ dBm.

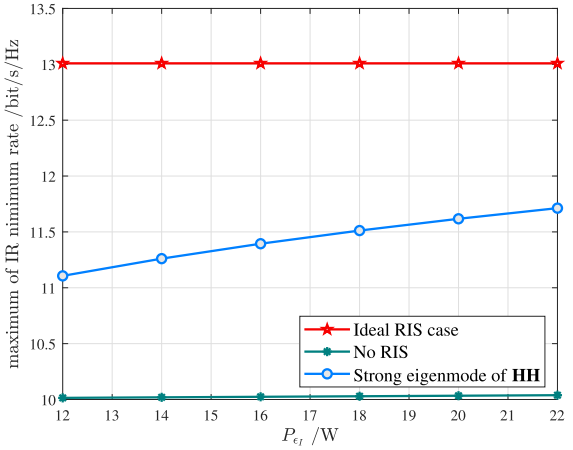

FIGURE 4. Maximum IR minimum rate over P_{ε_I} when $\sigma_n^2 = -130$ dBm.

i.i.d. Rayleigh distribution with zero mean. The RIS EH efficiency is $\xi = 1$. The maximum number of iterations of the proposed algorithm is set to 50. The transmit power at the APs is set to $P_{\varepsilon_I} \in [10, 30]$ dBm.

First, a plot of the maximum IR minimum rate over the feasible range of the ER energy bound P_{ε_I} is shown in Fig. 3 for $\sigma_n^2 = -140$dBm. We compared the behaviors in ideal RIS and imperfect RIS cases with beamforming. When the transmit power at the BS increases, the rate rapidly rises in all cases, which indicates the intuitive conclusion that increasing the transmit power is a straightforward way to improve the rate of an IR in the target network. Moreover, the behavior in the imperfect case improves more quickly than that under ideal circumstances, although there is still a gap between perfect and unsatisfactory conditions.

In Fig. 4, we assume $\sigma_n^2 = -130$dBm and compare the behaviors in RIS-aided, no RIS, and strong eigenmode of $\boldsymbol{HH}$ cases. In strong eigenmode of $\boldsymbol{HH}$ regime, the optimal transmission strategy is beamforming over the strongest eigenmode of the effective MIMO channel, by allocating all transmit power to the strongest eigenchannel. When the transmit power at the BS increases, the rate also increases in all states, similar to Fig. 3. Moreover, the behavior in the strong eigenmode of $\boldsymbol{HH}$ case updates more quickly than

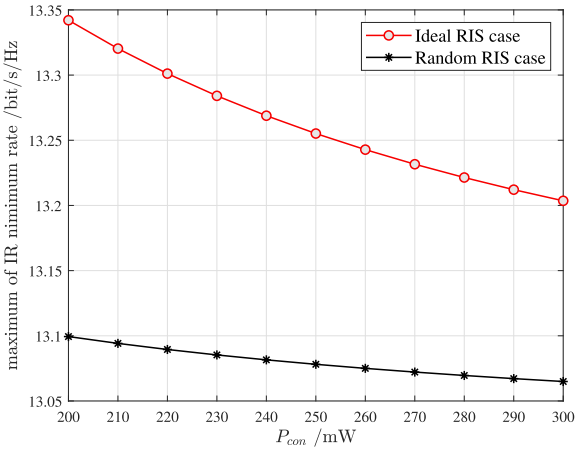

FIGURE 5. Maximum IR minimum rate over P_{con} when $\sigma_n^2 = -110$ dBm.

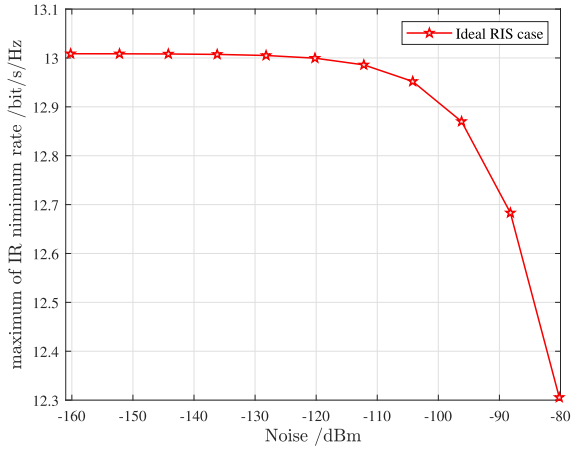

FIGURE 6. Maximum IR minimum rate over noise.

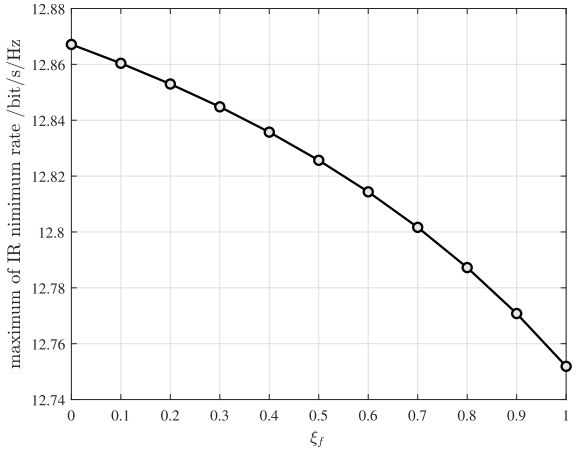

FIGURE 7. Maximum IR minimum rate change over ξ_f.

that under ideal circumstances. However, there is still a gap between the perfect RIS and strong eigenmode of $\boldsymbol{HH}$ cases, while the behavior under the no-RIS conditions is the worst.

A plot of the change in the maximum IR minimum rate over the feasible range of the total transmit power P_{con} is shown in Fig. 5 when $\sigma_n^2 = -110$dBm. We compare the behaviors in the ideal RIS case and random RIS case, and it is easy to conclude that the ideal RIS case achieves a better performance. The stronger the power constraints are, the lower the rate that can be achieved. This finding indicates that we must strike a balance between restricting the lowest consumption and the maximum IR minimum rate.

In Fig. 6, we show the behaviors in the RIS-aided cases over noise. When the noise is more considerable, the system has poorer performance. Fig. 7 shows the maximum IR minimum rate over the feasible range of the Frobenius norm-bounded uncertainty region size ξ_f. With the growth of the Frobenius norm, the rate performance worsens.

V. CONCLUSION

This paper investigates an RIS-assisted SWIPT system in wireless sensor networks from two different perspectives of channel conditions: perfect and imperfect channels. The corresponding maximum IR minimum rate is investigated as a nonconvex constrained optimization problem. Under optimal boundary and KKT conditions, the problem can be globally solved by the proposed SDP-based linear search method. In addition, the closed-form optimal solution is derived for an interference-free scenario with perfect CSI.

Finally, our simulation results show that the proposed algorithm can converge within a few iterations, and the numerical analysis provides practical insights into the effects of various system parameters, such as the ER energy bound, total transmit power, and Frobenius norm-bounded uncertainty region size.

APPENDIX A

$$\psi^*\bar{\boldsymbol{h}}_1^H\bar{\boldsymbol{h}}_1 + \frac{1}{\mu}\boldsymbol{h}\boldsymbol{h}^H + \lambda^*\boldsymbol{H}\boldsymbol{H}^H + \beta^*\boldsymbol{I}_N - \boldsymbol{Z}_{\boldsymbol{V}}^* = 0 \quad (31a)$$

$$\frac{1}{\mu}\boldsymbol{h}\boldsymbol{h}^H + \lambda^*\boldsymbol{H}\boldsymbol{H}^H + \beta^*\boldsymbol{I}_N - \boldsymbol{Z}_{\boldsymbol{Q}}^* = 0 \quad (31b)$$

$$\boldsymbol{Z}_{\boldsymbol{V}}^*\boldsymbol{V}^* = 0, \quad \boldsymbol{Z}_{\boldsymbol{Q}}^*\boldsymbol{Q}^* = 0 \quad (31c)$$

$$\boldsymbol{Z}_V \succeq 0, \quad \boldsymbol{Z}_Q \succeq 0 \quad (31d)$$

$$\lambda^*\Bigg(\eta_{i_E}\Big(\sum_{i_I\in\mathcal{K}_I}\mathrm{tr}(\boldsymbol{H}_{i_E}\boldsymbol{V}_{i_I}\boldsymbol{H}_{i_E}^H) + \sum_{i_E\in\mathcal{K}_E}\mathrm{tr}(\boldsymbol{H}_{i_E}\boldsymbol{Q}_{i_E}\boldsymbol{H}_{i_E}^H)\Big) - E_{con}\Bigg) = 0 \quad (31e)$$

$$\beta^*\left(\sum_{i_I\in\mathcal{K}_I}\|\boldsymbol{v}_{i_I}\|^2 + \sum_{i_E\in\mathcal{K}_E}\mathrm{tr}(\boldsymbol{Q}_{i_E}) - P_\varepsilon\right) = 0 \quad (31f)$$

$$\psi^*\left(\mu - \bar{\boldsymbol{h}}_1^H\boldsymbol{V}_{\bar{n}_1}\bar{\boldsymbol{h}}_1\right) = 0. \quad (31g)$$

Here, $\{\lambda, \beta, \psi\}$ are the nonnegative Lagrangian multipliers for constraints $\{CR1, CR2, CR3\}$.

By substituting (31c) into (31a) and (31b), we obtain $\psi^* = 0$, $\frac{\boldsymbol{h}\boldsymbol{h}^H}{\bar{\boldsymbol{h}}_1^H\boldsymbol{V}_{\bar{n}_1}\bar{\boldsymbol{h}}_1} + \lambda^*\boldsymbol{H}\boldsymbol{H}^H + \beta^*\boldsymbol{I}_N = 0$.

If $\beta^* = 0$, then $\sum_{i_I\in\mathcal{K}_I}\mathrm{tr}(\boldsymbol{H}_{i_E}\boldsymbol{V}_{i_I}\boldsymbol{H}_{i_E}^H) + \sum_{i_E\in\mathcal{K}_E}\mathrm{tr}(\boldsymbol{H}_{i_E}\boldsymbol{Q}_{i_E}\boldsymbol{H}_{i_E}^H) = E_{con}/\eta_{i_E}$.

Otherwise, $\beta^* > 0$, and $\sum_{i_I\in\mathcal{K}_I}\|\boldsymbol{v}_{i_I}\|^2 + \sum_{i_E\in\mathcal{K}_E}\mathrm{tr}(\boldsymbol{Q}_{i_E}) = P_\varepsilon$.

APPENDIX B

$$\frac{1}{\mu}(\widehat{\boldsymbol{h}}_{i_E}+\Delta\boldsymbol{h}_{i_E})(\widehat{\boldsymbol{h}}_{i_E}+\Delta\boldsymbol{h}_{i_E})^H+\left(\lambda^*+\psi^*\right)\mathbf{R}_E\mathbf{R}_E^H+\beta^*\boldsymbol{I}_N-\boldsymbol{Z}_{\boldsymbol{V}}^*=0 \tag{32a}$$

$$\frac{1}{\mu}(\widehat{\boldsymbol{h}}_{i_E}+\Delta\boldsymbol{h}_{i_E})(\widehat{\boldsymbol{h}}_{i_E}+\Delta\boldsymbol{h}_{i_E})^H+\lambda^*\mathbf{R}_E\mathbf{R}_E^H+\beta^*\boldsymbol{I}_N-\boldsymbol{Z}_{\boldsymbol{Q}}^*=0 \tag{32b}$$

$$\boldsymbol{Z}_{\boldsymbol{V}}^*\boldsymbol{V}^*=0,\quad \boldsymbol{Z}_{\boldsymbol{Q}}^*\boldsymbol{Q}^*=0 \tag{32c}$$

$$\boldsymbol{Z}_{\boldsymbol{V}}\geq 0,\quad \boldsymbol{Z}_{\boldsymbol{Q}}\geq 0 \tag{32d}$$

$$\beta^*\left(\sum_{i_I\in\mathcal{K}_I}\|\boldsymbol{v}_{i_I}\|^2+\sum_{i_E\in\mathcal{K}_E}\mathrm{tr}(\boldsymbol{Q}_{i_E})-P_\varepsilon\right)=0 \tag{32e}$$

$$\lambda^*\Bigg(\eta_{i_E}\sum_{i_I\in\mathcal{K}_I,i_E\in\mathcal{K}_E}(\widehat{\boldsymbol{H}}_{i_E}+\Delta\boldsymbol{H}_{i_E})^H\mathrm{tr}(\boldsymbol{V}_{i_I}+\boldsymbol{Q}_{i_E})(\widehat{\boldsymbol{H}}_{i_E}+\Delta\boldsymbol{H}_{i_E})-E_{con}\Bigg)=0 \tag{32f}$$

$$\psi^*\left(\mathbf{I}_{E_1}+\mathbf{R}_E^H\boldsymbol{V}_{\bar{n}_1}\mathbf{R}_E\right)=0. \tag{32g}$$

Here, $\{\lambda,\beta,\psi\}$ are the nonnegative Lagrangian multipliers for constraints $\{CR1, CR2, CR3\}$.

By substituting (32c) into (32a) and (32b), we obtain $\psi^*=0$.

If $\lambda^*=0$, $\beta^*=-\frac{1}{\mu}(\widehat{\boldsymbol{H}}_{i_E}+\Delta\boldsymbol{H}_{i_E})(\widehat{\boldsymbol{H}}_{i_E}+\Delta\boldsymbol{H}_{i_E})^H$, and $\mathbf{R}_E^H(\boldsymbol{V}_{i_J}+\boldsymbol{Q}_{i_E})\mathbf{R}_E=\mathbf{I}_{E_1}$, then $\psi^*=0$. This means that the constraint is not tight in the optimum conditions.

Otherwise, $\lambda^*>0$, and $(\widehat{\boldsymbol{H}}_{i_E}+\Delta\boldsymbol{H}_{i_E})^H(\mathrm{tr}(\boldsymbol{V})+\mathrm{tr}(\boldsymbol{Q}))(\widehat{\boldsymbol{H}}_{i_E}+\Delta\boldsymbol{H}_{i_E})=E_{con}/\eta_{i_E}$. Then, we obtain the closed-form solution of (23a).

REFERENCES

[1] J. Guo, S. Durrani, X. Zhou, and H. Yanikomeroglu, "Outage probability of ad hoc networks with wireless information and power transfer," *IEEE Wireless Commun. Lett.*, vol. 4, no. 4, pp. 409–412, Aug. 2015.
[2] S. Guo, F. Wang, Y. Yang, and B. Xiao, "Energy-efficient cooperative transmission for simultaneous wireless information and power transfer in clustered wireless sensor networks," *IEEE Trans. Commun.*, vol. 63, no. 11, pp. 4405–4417, Nov. 2015.
[3] W. Lu, Y. Gong, J. Wu, H. Peng, and J. Hua, "Simultaneous wireless information and power transfer based on joint subcarrier and power allocation in OFDM systems," *IEEE Access*, vol. 5, pp. 2763–2770, 2017.
[4] W. Wang, R. Wang, H. Mehrpouyan, N. Zhao, and G. Zhang, "Beamforming for simultaneous wireless information and power transfer in two-way relay channels," *IEEE Access*, vol. 5, pp. 9235–9250, 2017.
[5] Z. Yang, Z. Ding, P. Fan, and G. K. Karagiannidis, "Outage performance of cognitive relay networks with wireless information and power transfer," *IEEE Trans. Veh. Technol.*, vol. 65, no. 5, pp. 3828–3833, May 2016.
[6] L. R. Varshney, "Transporting information and energy simultaneously," in *Proc. IEEE Int. Symp. Inf. Theory*, Jul. 2008, pp. 1612–1616.
[7] T. D. P. Perera, D. N. K. Jayakody, S. K. Sharma, S. Chatzinotas, and J. Li, "Simultaneous wireless information and power transfer (SWIPT): Recent advances and future challenges," *IEEE Commun. Surveys Tuts.*, vol. 20, no. 1, pp. 264–302, 1st Quart., 2018.
[8] X. Wang, W. Feng, Y. Chen, Z. Chu, and N. Ge, "Energy-efficiency maximization for secure multiuser MIMO SWIPT systems with CSI uncertainty," *IEEE Access*, vol. 6, pp. 2097–2109, 2017.
[9] R. Zhang, R. G. Maunder, and L. Hanzo, "Wireless information and power transfer: From scientific hypothesis to engineering practice," *IEEE Commun. Mag.*, vol. 53, no. 8, pp. 99–105, Aug. 2015.
[10] C. Pan, H. Ren, K. Wang, M. Elkashlan, A. Nallanathan, J. Wang, and L. Hanzo, "Intelligent reflecting surface aided MIMO broadcasting for simultaneous wireless information and power transfer," *IEEE J. Sel. Areas Commun.*, vol. 38, no. 8, pp. 1719–1734, Aug. 2020.
[11] Q. Wu, G. Y. Li, W. Chen, D. W. K. Ng, and R. Schober, "An overview of sustainable green 5G networks," *IEEE Wireless Commun.*, vol. 24, no. 4, pp. 72–80, Aug. 2017.
[12] Q. Wu and R. Zhang, "Intelligent reflecting surface enhanced wireless network via joint active and passive beamforming," *IEEE Trans. Wireless Commun.*, vol. 18, no. 11, pp. 5394–5409, Nov. 2019.
[13] S. Zhang, Q. Wu, S. Xu, and G. Y. Li, "Fundamental green tradeoffs: Progresses, challenges, and impacts on 5G networks," *IEEE Commun. Surveys Tuts.*, vol. 19, no. 1, pp. 33–56, 1st Quart., 2017.
[14] H. Xing, L. Liu, and R. Zhang, "Secrecy wireless information and power transfer in fading wiretap channel," *IEEE Trans. Veh. Technol.*, vol. 65, no. 1, pp. 180–190, Jan. 2016.
[15] M. Zhang, Y. Liu, and R. Zhang, "Artificial noise aided secrecy information and power transfer in OFDMA systems," *IEEE Trans. Wireless Commun.*, vol. 15, no. 4, pp. 3085–3096, Apr. 2016.
[16] M. Cui, G. Zhang, and R. Zhang, "Secure wireless communication via intelligent reflecting surface," *IEEE Wireless Commun. Lett.*, vol. 8, no. 5, pp. 1410–1414, Oct. 2019.
[17] J. Chen, Y.-C. Liang, Y. Pei, and H. Guo, "Intelligent reflecting surface: A programmable wireless environment for physical layer security," *IEEE Access*, vol. 7, pp. 82599–82612, 2019.
[18] H. Shen, W. Xu, S. Gong, Z. He, and C. Zhao, "Secrecy rate maximization for intelligent reflecting surface assisted multi-antenna communications," *IEEE Commun. Lett.*, vol. 23, no. 9, pp. 1488–1492, Sep. 2019.
[19] X. Zhou, Q. Wu, S. Yan, F. Shu, and J. Li, "UAV-enabled secure communications: Joint trajectory and transmit power optimization," *IEEE Trans. Veh. Technol.*, vol. 68, no. 4, pp. 4069–4073, Apr. 2019.
[20] X. Guan, Q. Wu, and R. Zhang, "Intelligent reflecting surface assisted secrecy communication: Is artificial noise helpful or not?" *IEEE Wireless Commun. Lett.*, vol. 9, no. 6, pp. 778–782, Jun. 2020.
[21] Z. Chu, W. Hao, P. Xiao, and J. Shi, "Intelligent reflecting surface aided multi-antenna secure transmission," *IEEE Wireless Commun. Lett.*, vol. 9, no. 1, pp. 108–112, Jan. 2020.
[22] C. Pan, H. Ren, K. Wang, W. Xu, M. Elkashlan, A. Nallanathan, and L. Hanzo, "Multicell MIMO communications relying on intelligent reflecting surfaces," *IEEE Trans. Wireless Commun.*, vol. 19, no. 8, pp. 5218–5233, Aug. 2020.
[23] B. Zheng, Q. Wu, and R. Zhang, "Intelligent reflecting surface-assisted multiple access with user pairing: NOMA or OMA?" *IEEE Commun. Lett.*, vol. 24, no. 4, pp. 753–757, Apr. 2020.
[24] J. Zhao, "A survey of intelligent reflecting surfaces (IRSs): Towards 6G wireless communication networks," 2019, *arXiv:1907.04789*. [Online]. Available: http://arxiv.org/abs/1907.04789
[25] Q. Wu and R. Zhang, "Weighted sum power maximization for intelligent reflecting surface aided SWIPT," *IEEE Wireless Commun. Lett.*, vol. 9, no. 5, pp. 586–590, May 2020.
[26] J. D. Griffin and G. D. Durgin, "Complete link budgets for backscatter-radio and RFID systems," *IEEE Antennas Propag. Mag.*, vol. 51, no. 2, pp. 11–25, Apr. 2009.

ZIYI YANG received the B.S. degree in electronic engineering from Beijing Institute of Technology, Beijing, China, in 2015, where she is currently pursuing the Ph.D. degree with the School of Electronic and Information. Her research interests include signal processing, convex optimization, massive MIMO systems, and wireless communications.

YU ZHANG received the B.S. degree in electrical engineering from the University of Electronic Science and Technology of China, in 1995, the M.S. degree in electrical engineering from Beijing Institute of Technology, in 1997, and the Ph.D. degree in electrical engineering from Peking University, in 2001. He is currently an Assistant Professor with the School of Information and Electronics, Beijing Institute of Technology. His research interests include communications, the Internet of Things, and space-based networks.